Journal of Ayurveda and Integrative Medicine 12 (2021) 465–473

Contents lists available at ScienceDirect

Journal of Ayurveda and Integrative Medicine

journal homepage: http://elsevier.com/locate/jaim

Original Research Article (Experimental)

Intervention by picroside II on FFAs induced lipid accumulation and lipotoxicity in HepG2 cells

Hiteshi Dhami-Shah [a, b, c, *], Rama Vaidya [a], Manasi Talwadekar [b], Eisha Shaw [b], Shobha Udipi [a], Ullas Kolthur-Seetharam [b], Ashok D.B. Vaidya [a]

[a] Medical Research Centre of Kasturba Health Society, Division of Endocrine and Metabolic Disorders, 17 KD Road, Vile Parle West, Mumbai, 400056, Maharashtra, India
[b] Tata Institute of Fundamental Research, Department of Biological Science, Homi Bhabha Road, Navy Nagar, Colaba, Mumbai, 400005, Maharashtra, India
[c] S.N.D.T University, Department of Food Science and Nutrition, Juhu Road, Santacruz (west), Mumbai, 400049, Maharashtra, India

ARTICLE INFO

Article history:
Received 7 May 2020
Received in revised form
10 March 2021
Accepted 10 April 2021
Available online 2 August 2021

Keywords:
NAFLD
Picrorhiza kurroa
Picroside II
Reverse pharmacology

ABSTRACT

Background: Accumulation of free fatty acids (FFAs) in hepatocytes is a hallmark of liver dysfunction and non-alcoholic fatty liver disease (NAFLD). Excessive deposition of FFAs alters lipid metabolism pathways increasing the oxidative stress and mitochondrial dysfunction. Attenuating hepatic lipid accumulation, oxidative stress, and improving mitochondrial function could provide potential targets in preventing progression of non-alcoholic fatty liver (NAFL) to non-alcoholic steatohepatitis (NASH). Earlier studies with *Picrorhiza kurroa* extract have shown reduction in hepatic damage and fatty acid infiltration in several experimental models and also clinically in viral hepatitis. Thus, the effect of *P. kurroa's* phytoactive, picroside II, needed mechanistic investigation in appropriate *in vitro* liver cell model.
Objective(s): To study the effect of picroside II on FFAs accumulation, oxidative stress and mitochondrial function with silibinin as a positive control in *in vitro* NAFLD model.
Materials and methods: HepG2 cells were incubated with FFAs-1000μM in presence and absence of Picroside II-10 μM for 20 hours.
Results: HepG2 cells incubated with FFAs-1000μM lead to increased lipid accumulation. Picroside II-10μM attenuated FFAs-induced lipid accumulation (33%), loss of mitochondrial membrane potential ($\Delta\Psi m$), ATP depletion, and production of reactive oxygen species (ROS). A concomitant increase in cytochrome C at transcription and protein levels was observed. An increase in expression of MnSOD, catalase, and higher levels of tGSH and GSH:GSSG ratios underlie the ROS salvaging activity of picroside II.
Conclusion: Picroside II significantly attenuated FFAs-induced-lipotoxicity. The reduction in ROS, increased antioxidant enzymes, and improvement in mitochondrial function underlie the mechanisms of action of picroside II. These findings suggest a need to develop an investigational drug profile of picroside II for NAFLD as a therapeutic strategy. This could be evaluated through the fast-track path of reverse pharmacology.

1. Introduction

Non-alcoholic fatty liver disease (NAFLD) is caused by the accumulation of fat within the hepatocytes (>5.5%) in the absence of significant alcohol intake [1]. NAFLD is primarily seen in patients having features of metabolic syndrome (MS) such as hypertension, dyslipidemia, insulin resistance (IR) with or without impaired glucose tolerance and visceral obesity [2]. It covers a spectrum of disorders beginning with benign steatosis (NAFL) to non-alcoholic steatohepatitis (NASH), which may progress to fibrosis, cirrhosis and cancer in some patients [3]. Today, ≥30% of adults and 10% of children are globally affected by NAFLD [4]. Delaying the progression of NAFL to NASH at an earlier stage with safe intervention via natural drug therapies would therefore be worth exploring.

* Corresponding author.
E-mail: hiteshi.dhami@gmail.com
Peer review under responsibility of Transdisciplinary University, Bangalore.

https://doi.org/10.1016/j.jaim.2021.04.007

In NAFL, the deposition of free fatty acids (FFAs) and triglycerides (TGs) are caused by an increase in fatty acid uptake, lipogenesis and a concomitant decrease in VLDL-TG secretion [5]. Elevation in inflammation and oxidative stress is seen during the progression of NAFL to NASH [6]. Oxidative stress contributes to the production of reactive oxygen species, lipid peroxidation products and decreases the levels of antioxidants such as superoxide dismutase, glutathione, and catalase. Impairment in mitochondrial function and ATP generation is also observed. All these factors aggravate inflammation and cell death [7,8].

Apart from lifestyle modifications, optimal control of risk factors with antioxidants, anti-diabetic drugs and statins form an integral part of the management of NAFLD until specific targeted therapies are available to prevent the progression of NASH and fibrosis. Currently, there is a need for safe and natural therapeutic interventions in the early stages of NAFLD [9]. Over the past few years, the therapeutic potential of medicinal plants used in traditional systems has gained increased attention. *Picrorhiza kurroa* is one of the medicinal plants known for its clinical and experimental hepatoprotective activity [10]. Our group has shown *P. kurroa's*, hepatoprotective efficacy in a placebo-controlled trial in patients with viral hepatitis. The extracts *of P. kurroa* significantly reduced hepatic fatty infiltration induced by CCl_4, galactosamine, paracetamol, thioacetamide, and high-fat diet in rat models [11–17]. *P. kurroa* extract contains high levels of phytoactives such as picroside I, II, III, and apocynin. Recently, our group studied the effect of picroside I and II on the fatty acid accumulation in an *in vitro* NAFLD model. Picroside II effectively attenuated the fatty acid accumulation in HepG2 cells via decreasing FFAs uptake and lipogenesis. Picroside I on the other hand, did not show any effect on fatty acid accumulation in HepG2 cells. Since the study aimed at examining the inhibitory activity of the phytoactives on lipid accumulation, picroside I was discontinued from further analysis [18].

In the present study, the effect of FFAs on oxidative stress, ATP production, and mitochondrial function was examined along with the potential of picroside II in attenuating FFAs-induced-lipotoxicity.

2. Materials and methods

2.1. Culturing of HepG2 cell line

HepG2 cells (AddexBio Technologies, USA) were cultured in Dulbecco's Modified Eagle Medium (HiMeida, India) with 10% fetal bovine serum (Gibco Life Technologies, USA) and 1% trypsin–EDTA, antibiotic-antimycotic solution (Himedia, India). Cells were maintained in a humidified incubator in 5% CO_2 at 37 °C (Thermo Scientific, USA). All experiments were performed when the cells reached ~75–80% confluence. The experiments were repeated four times.

2.2. Preparing FFA – bovine serum albumin (BSA) conjugate

Long-chain FFAs viz., palmitic acid (Sisco Research Laboratories Pvt Ltd, India) and oleic acids (Sigma, India) were conjugated individually with BSA (Sisco Research Laboratories Pvt Ltd, India). FFAs-BSA conjugate was prepared as previously described in the protocol [19]. Briefly, 100 mM stock of FFA was prepared in 0.1 N NaOH at 70 °C in a thermomixer (Eppendorf, USA). A 5% (wt/vol) BSA solution was prepared in double-distilled water. Since FFAs were conjugated with 5% BSA, control cells were also treated with 5% BSA. A 10 mM FFAs-BSA conjugate was prepared by complexing appropriate amount of FFA to 5% BSA solution in a water-bath at 55 °C and filtered using 0.45 μm pore size polyvinylidene fluoride hydrophilic membrane filter. The conjugate was cooled to room temperature and stored at −20 °C. At this temperature, it was found to be stable for 3–4 weeks. As FFAs were conjugated with 5% BSA, the control cells were also treated with 5% BSA.

2.3. Cell cytotoxicity detection

HepG2 cells were treated with different concentrations of FFAs, oleic and palmitic acid in a ratio 2:1 (250–2000 μM), picroside I and II (3–300 μM) (Natural Remedies Pvt Ltd, India, HPLC purity 97.9%), and silibinin (3–300 μM) (Sigma–Aldrich, USA, HPLD purity 98%) for 24 h. Post-treatment, the cells were incubated with 5 mg/mL of methyl thiazolyl tetrazolium (MTT) (Sigma–Aldrich, India) for 4 h. The blue coloured formazan crystals formed were dissolved in DMSO and absorbance was measured at 570 nm (Biorad Elisa Reader 680) [20].

2.4. Colorimetric determination of lipid content with Oil Red O (ORO) staining

HepG2 cells were incubated with FFAs for 20 h and pre-incubated with phytoactives for 2 h prior to FFAs treatment. After treatment, the cells were fixed (4% formaldehyde) and stained with ORO solution (Sigma Aldrich – O0625, India) (3 mg/mL in 60% isopropanol) for 5 min. The lipid accumulation was quantified by measuring the absorbance of the extracted solution at 490 nm (PerkinElmer Multimode Plate Reader, Enspire) [21].

2.5. Determination of reactive oxygen species (ROS)

Intracellular ROS was measured using 2′, 7′-dichlorofluorescein (DCFH2-DA), (Sigma Aldrich, USA). Briefly, the treated cells were incubated with 40 nM of DCFH2-DA for 10 min and later washed, lysed, and centrifuged at 13,000 g for 5 min at 4 °C. The fluorescence intensity was measured in the supernatant of the samples (Tecan infinite M200 pro, Switzerland) at excitation 488 nm and emission 529 nm [22].

2.6. Estimation of total glutathione

The treated cells were washed and harvested in extraction buffer (0.1 Trition-X 100 and 0.6% sulfosalicylic acid in 0.1 M potassium phosphate buffer, pH 7.5), homogenized, and centrifuged at 3000 g for 10 min at 4 °C. The supernatant of the samples was incubated with Ellman's reagent (Sigma Aldrich, India) and glutathione reductase (Sigma Aldrich, India) for 10 min to allow for the conversion of glutathione disulfide to glutathione (GSSG to GSH). The sample was later incubated with β-$NADPH_2$ (Sigma Aldrich, India) for 1 min. The absorbances of the samples were read at 412 nm in a microplate reader using a kinetic program which monitored the reaction at 1 min interval for 10 min [23]. The concentration of total glutathione (tGSH) was determined from the samples using the standard curve of GSH (Sigma Aldrich, India). The values were expressed as tGSH μM/mg of protein.

2.7. Estimation of GSH to GSSG ratio

The treated cells were harvested in extraction buffer, (0.1% Trition-X 100 and 0.6% sulfosalicylic acid in 0.1 M potassium phosphate buffer, pH 7.5) homogenized, and centrifuged at 3000 g for 10 min at 4 °C. In order to measure GSSG (Sigma Aldrich, India) in a sample containing both GSH and GSSG by enzymatic method, free GSH was first masked. The cell extracts were treated with 2-vinylpyridine which covalently reacts with GSH and not GSSG to block it. The excess 2-vinylpyridine (Sigma Aldrich, India) was neutralized with triethanolamine (Sigma Aldrich, India). Once GSSG and tGSH levels were determined, GSH was calculated for

determination of GSH to GSSG ratio. tGSH was measured as described above. The concentration of GSH was calculated by the following formula: total glutathione ≈ GSH + 2 GSSG [24]. The ratio of GSH–GSSG was determined from values of GSH and GSSG μM/mg of protein.

2.8. ATP measurement

The treated cells were analyzed for ATP levels using ATPlite Detection Assay System (Molecular Probes, USA) as per the manufacturer's instructions [25]. Briefly, the cells were lysed, and the supernatant was collected after centrifugation at 13,000 g for 10 min at 4 °C. Luciferase activity was measured in a bioluminescence plate with 10 μL of supernatant and 90 μL of ATP reaction solution.

2.9. Mitochondrial membrane potential ($\Delta\Psi m$)

ΔΨm was measured using tetramethylrhodamine methyl ester (TMRM), (Thermo scientific, India). The treated cells were incubated with 10 nM of TMRM for 5 min at 37 °C, 5% CO_2. Later, the cells were trypsinized, collected, and washed once in 1 × PBS. The cells were assayed for TMRM fluorescence using flow cytometry (BD LSRFortessa cell analyzer, Belgium) [26].

2.10. Quantitative RT-PCR

The treated cells were lysed using 1 mL Trizol reagent (Thermo scientific, India). Total RNA was isolated and complementary DNAs (cDNAs) were synthesized using cDNA reverse transcription kit as per manufacturer instructions using PCR thermal cycler (Applied Biosystems, USA). Quantitative detection of Manganese superoxide dismutase (MnSOD), Catalase, Cytochrome C, transcription factor A mitochondrial (TFAM), Cytochrome *c* oxidase IV (COX IV), and β-actin was undertaken. A primer sequence of each gene synthesized by Sigma–Aldrich, India was used as mentioned in Table 1. RT-PCR amplification was performed in the total volume of 20 μL, comprising 10 μL SYBR Green (2x), 1 μL each of forward and reverse primer (10 μM), 4 ul nuclease-free water and 4 μL cDNA solution. PCR was run for 35 cycles using ABI-7500 Fast RT-PCR system. The conditions used were denaturation at 95 °C for 5 min, 35–40 cycles of 95 °C for 15 s, annealing at 60 °C for 1 min, extension at 72 °C for 1 min, and a final extension at 72 °C for 5 min. The Ct value of each gene was normalized with β-actin [27].

2.11. Western blot

HepG2 treated cells were harvested in RIPA buffer (50 mM Tris pH8.0, 150 mM NaCl, 0.1%SDS, 0.02% Sodium azide, 1% NP40, 0.5% Sodium deoxycholate) supplemented with protease and phosphatase inhibitor cocktails (Sigma–Aldrich, USA). Protein was quantified using BCA protein assay kit (Thermo Fisher Scientific, USA). SDS-PAGE was performed using 40 μg of protein sample on a 10% denaturing SDS gel and transferred on polyvinylidene fluoride membrane (Bio-Rad, California, USA). Each blot was incubated with specific anti-Cytochrome C (Abcam, USA) (dilution 1:1000), anti-TFAM (Abcam USA) (dilution 1:1000), anti-COX IV (Santacruz Biotechnology, USA) (1:200), and anti-tubulin (Sigma Aldrich, India) (dilution 1:1000) followed by a secondary. The blot images were captured using ChemiDoc™ XRS (GE Amersham Imager, USA). The blot intensity was quantified using Image J software and the results were reported relative to tubulin band density used as a load control [28].

2.12. Statistical analysis

The software package GraphPad (version 5.0, Prism, CA, USA) was used for analysis. A minimum of four to six independent experiments were carried out and the standard error of the mean (SEM) was derived. Statistical significance was determined using one and two way analysis of variance (ANOVA), where p value $< 0.05^{(*)}$, $<0.01^{(**)}$, $<0.001^{(***)}$ was considered to be statistically significant.

3. Results

3.1. FFAs induced hepatic steatosis cell model

As per the previous study, the cell culture model of hepatic steatosis was established by loading HepG2 cells with FFAs mixture of OA: PA/2:1 [18]. The concentration range selected for standardizing the model was 250–2000 μM. The microscopic examination showed lipid accumulation within the cytoplasm of HepG2 cells loaded with lipids. In order to determine the appropriate cell culture concentration for steatosis model, MTT was used to estimate the number of viable cells. FFAs mixture did not affect the cell viability in the concentration range of 250–500 μM as compared to control cells. At FFAs concentration of 1000 μM, a 10% reduction was observed in cell viability. However, at FFAs mixture of 2000 μM, there was a significant reduction in cell viability of about 35.73%, $p < 0.001$ (Fig. 1A). Since the FFAs concentration of 2000 μM was found to be cytotoxic, concentration of 1000 μM was used for further studies. Also, the decrease in cell viability correlated with increase in ROS production in a dose-dependent manner (Fig. 1B).

The lipid accumulation in HepG2 was quantified by treating the cells with FFAs in a concentration range of 250–1000 μM. The lipid accumulation was confirmed using ORO stain. Post-treatment, the colorimetric quantification showed a dose–dependent rise in lipid accumulation. The percent accumulation of FFAs was found to be

Table 1
Primer sequence used in the study for HepG2 cell line.

Gene	Pathway	Sequence (5 → 3)	Gene Bank no./ref
Human MnSOD	Antioxidant enzymes	Forward: CCTGGAACCTCACATCAACG Reverse: GCTATCTGGGCTGTAACATCTC	NM_000636.4
Human Catalase	Antioxidant enzymes	Forward: CAGATAGCCTTCGACCCAAG Reverse:GTAGGGACAGTTCACAGGTATATG	NM_001752.4
Human Cytochrome *c*	Transcription factors affecting mitochondrial biogenesis	Forward: GTGCCACACCGTTGAAAAG Reverse: AGTGTATCCTCTCCCCAGATG	NM_018947.5
Human TFAM		Forward: TTTCTCCGAAGCATGTGGG Reverse: GCCAAGACAGATGAAAACCAC	NM_003201.3
Human COX IV		Forward: GCACTGAAGGAGAAGGAGAAG Reverse: CCACAACCGTCTTCCACTC	NM_001861.5
Human β-actin	Housekeeping gene	Forward: GTCTTCCCCTCCATCGT Reverse: CGTCCCCACATGGAAT	NM_007393.5

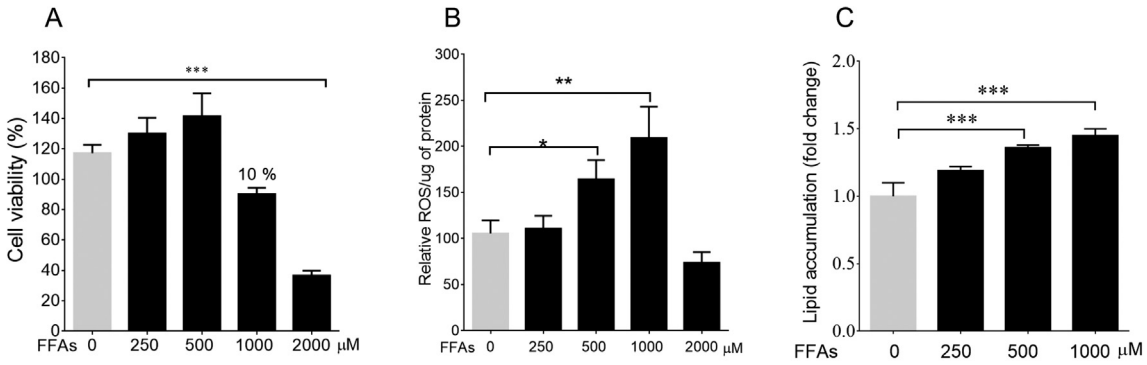

Fig. 1. FFAs induced lipid accumulation and cytotoxicity in HepG2 cells: The cell viability of FFAs was measured using MTT. FFAs – 2000 µM shows toxicity vs control cells $*p < 0.05$ (A). FFAs-500 µM and FFAs-1000 µM induced ROS versus control cells, $*p < 0.05$ and $**p < 0.001$ (B). The colorimetric quantification of FFAs loaded cells using ORO stain, FFAs – 500 µM and FFAs – 1000 µM vs control cells $***p < 0.001$ (C). The values are expressed as mean ± SEM, N = 4, n = 3.

15%, 25.6%, and 32.3% at 250, 500 and 1000 µM respectively (Fig. 1C). The concentration of FFAs showing the highest accumulation i.e., 1000 µM, was chosen in the study for further analysis. The effect of phytoactives, picroside II, and silibinin, on lipid accumulation was examined at FFAs-1000 µM.

3.2. Picroside II reduces lipid accumulation in FFA treated HepG2 cells

Prior to investigating the effect of picroside II and silibinin on lipid accumulation, its response was tested on cell proliferation and cytotoxicity using MTT. Notably, picroside II did not affect the cell viability in the concentration range of 3–100 µM (Fig. 2A). It was interesting to observe that silibinin too, did not show toxicity in the concentration range of 3–100 µM (Fig. 2B), as demonstrated earlier [29]. For both the phytoactives, picroside II and silibinin, an optimal concentration of 10 µM was selected for further analysis. The phytoactives were pre-treated 2 h prior to loading of FFAs on HepG2 cells. The microscopic examination of picroside II treated cells showed a remarkable decrease in intracellular lipid accumulation. The ORO colorimetric quantification supported the reduction in lipid accumulation. A 33% decrease in lipid accumulation with picroside II treatment was observed in FFAs loaded cells, $p < 0.01$ (Fig. 2C and D). Concomitantly, even silibinin showed 32% reduction in lipid accumulation in FFAs-loaded HepG2 cells, $p < 0.01$.

3.3. Picroside II ameliorates oxidative stress

Oxidative stress is a key pathologenetic mechanism in NAFLD contributing to hepatic injury [30]. To measure FFAs–induced

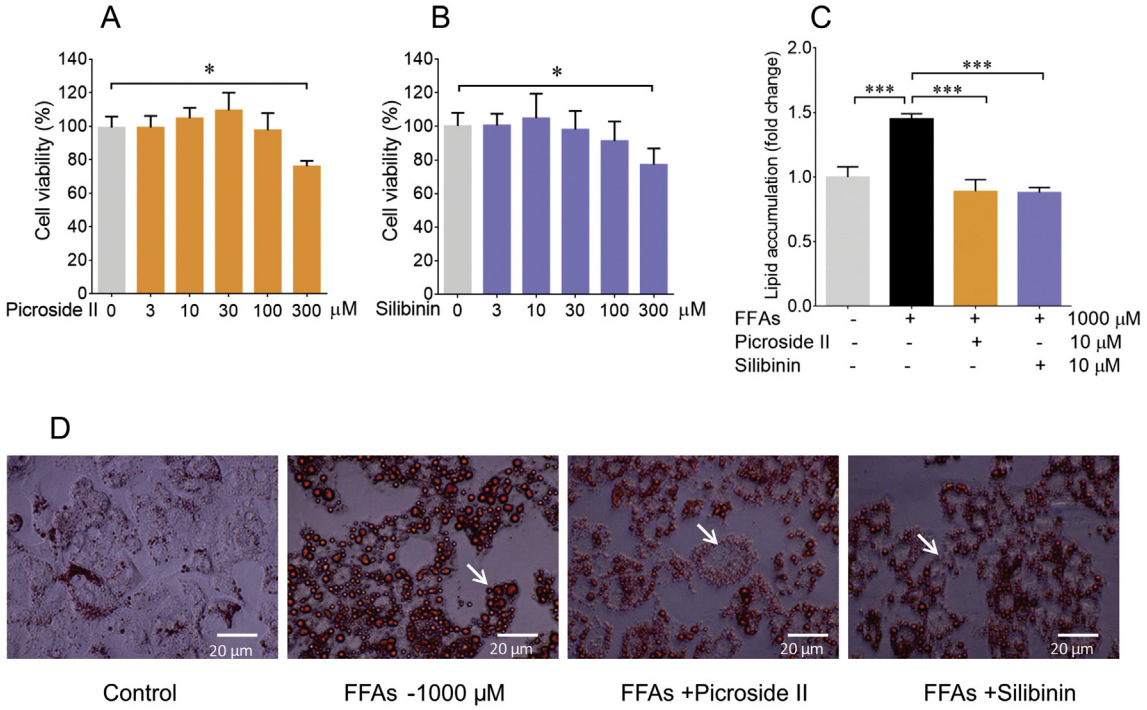

Fig. 2. Picroside II attenuates lipid accumulation in FFAs loaded cells: The cytotoxic effect of picroside II at 300 µM vs control cells $*p < 0.05$ (A) and Silibinin (positive control) at 300 µM vs control cells $*p < 0.05$ (B). HepG2 cells were pre-treated with picroside II and silibinin at a concentration of 10 µM for 2 h, followed by FFAs - 1000 µM challenge for another 20 h. Microscopic representation of the inhibitory effects of picroside II, and silibinin on FFAs accumulation using ORO stain (C). Quantification of lipid accumulation with ORO colorimetric assay, picroside II vs FFAs – 1000 µM $**p < 0.01$ and silibinin vs FFAs –1000 µM $*p < 0.05$ (D). The values are expressed as mean ± SEM, N = 4, n = 3.

oxidative stress, we measured total ROS production within FFAs-loaded HepG2 cells. The FFAs treatment of 1000 μM caused significant production of ROS within the cells. On loading with FFAs, the increase in ROS production was 97.9%, $p < 0.05$ (Fig. 3A) vs control cells. The increase in ROS formation was attenuated significantly by picroside II pre-treatment $p < 0.05$. Picroside II and silibinin caused a 38.3% and 37.8% decrease in ROS formation respectively. An increase in ROS formation was accompanied by decrease in the levels of glutathione, MnSOD and Catalase [31]. The antioxidant enzymes (MnSOD and Catalase) prevent oxidative damage by quenching ROS and decreasing the production of hydrogen peroxide. In the present study, there was a decrease in total glutathione levels on FFAs-loading suggesting glutathione depletion, $p < 0.01$. However, with FFAs-loading at 1000 μM, there was no change in the mRNA expression of MnSOD, Catalase, and the GSH:GSSG ratio vs the control. Picroside II was found to significantly rescue glutathione depletion in the FFAs loaded cells, $p < 0.05$ (Fig. 3B and C). Picroside II was also found to significantly increase the mRNA expression of MnSOD and Catalase by 1.5 fold, $p < 0.01$ (Fig. 3D and E). Silibinin did not have any effect on GSH:GSSG, MnSOD and Catalase.

3.4. Mitochondrial dysfunction is rescued by picroside II

Mitochondria are the major sites for ROS formation. Also, an increase in ROS formation is indicative of mitochondrial dysfunction. Mitochondrial dysfunction leads to a decrease in ATP production and ΔΨm [32]. In order to investigate the effect of FFAs loading in HepG2 cells on mitochondrial function, ATP levels were first determined. They were found to be reduced with FFAs treatment. FFAs caused a 48.84% decrease in ATP levels, $p < 0.01$ (Fig. 4A). Further, the reduction in ATP was prevented by picroside II and silibinin treatment, $p < 0.01$. Following the ATP levels, the ΔΨm was assayed in the FFAs-loaded HepG2 cells. FFAs caused a notable loss in ΔΨm, $p < 0.001$ (Fig. 4B). The loss in ΔΨm was reversed by picroside II and silibinin, $p < 0.05$. Additionally, decrease in the expression of Cytochrome C was seen on the FFAs-loading vs the control cells, $p < 0.05$ (Fig. 4C). No changes were observed in the protein expression of Cytochrome C in FFAs loaded cells compared to the control cells (Fig. 4D and E). Picroside II supplementation caused an increase in the mRNA and protein expression of Cytochrome C, $p < 0.05$. On the other hand, silibinin increased only the mRNA expression of Cytochrome C, $p < 0.05$. The effect of the FFAs-loading was analyzed on the mRNA and protein expression of COX IV and TFAM. Though, there were no changes observed in the mRNA and protein levels of COX IV and TFAM in FFAs-loaded cells v/s the control cells (Fig. S1A–F), picroside II and silibinin treatment led to an increase in the mRNA expression of COX IV, $p < 0.01$ and $p < 0.05$ respectively.

4. Discussion

Oxidative stress and mitochondrial dysfunction play a significant role in the progression of NAFL to NASH. The effects of FFAs-loading were studied on ROS generation, antioxidant enzymes, and mitochondrial function in HepG2 cells. HepG2 cells were loaded with FFAs mixture of oleic and palmitic acid in 2:1 ratio [18]. In the present study, a dose-dependent rise in the lipid accumulation at FFAs −1000 μM caused a significant increase in the ROS production.

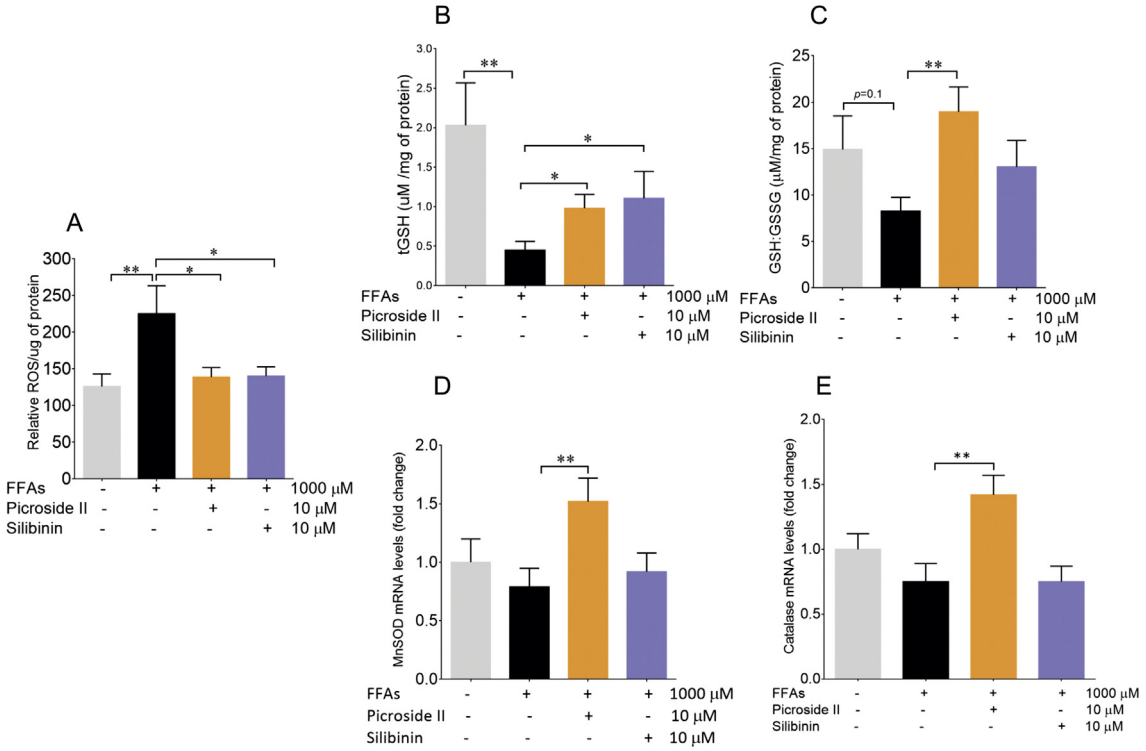

Fig. 3. Picroside II decreases oxidative stress in FFAs treated cells: HepG2 cells were pre-treated with picroside II and silibinin at a concentration of 10 μM for 2 h, followed by FFAs - 1000 μM challenge for another 20 h. The total ROS was measured using DCFDA stain, FFAs-1000 μM vs control $^{**}p < 0.01$, picroside II vs FFAs − 1000 μM $^{*}p < 0.05$ and silibinin vs FFAs - 1000 μM $^{*}p < 0.05$ (A). Estimation of tGSH levels on FFAs-1000 μM vs control $^{**}p < 0.01$, picroside II vs FFAs − 1000 μM, $^{*}p < 0.05$ and silibinin vs FFAs − 1000 μM, $^{*}p < 0.05$ (B). Estimation of GSH:GSSG ratio, picroside II vs FFAs − 1000 μM $^{*}p < 0.05$ (C). RT-PCR analysis of MnSOD (D) and Catalase (E), picroside II vs FFAs − 1000 μM, $^{*}p < 0.05$. The values are expressed as mean ± SEM, N = 4,n = 3.

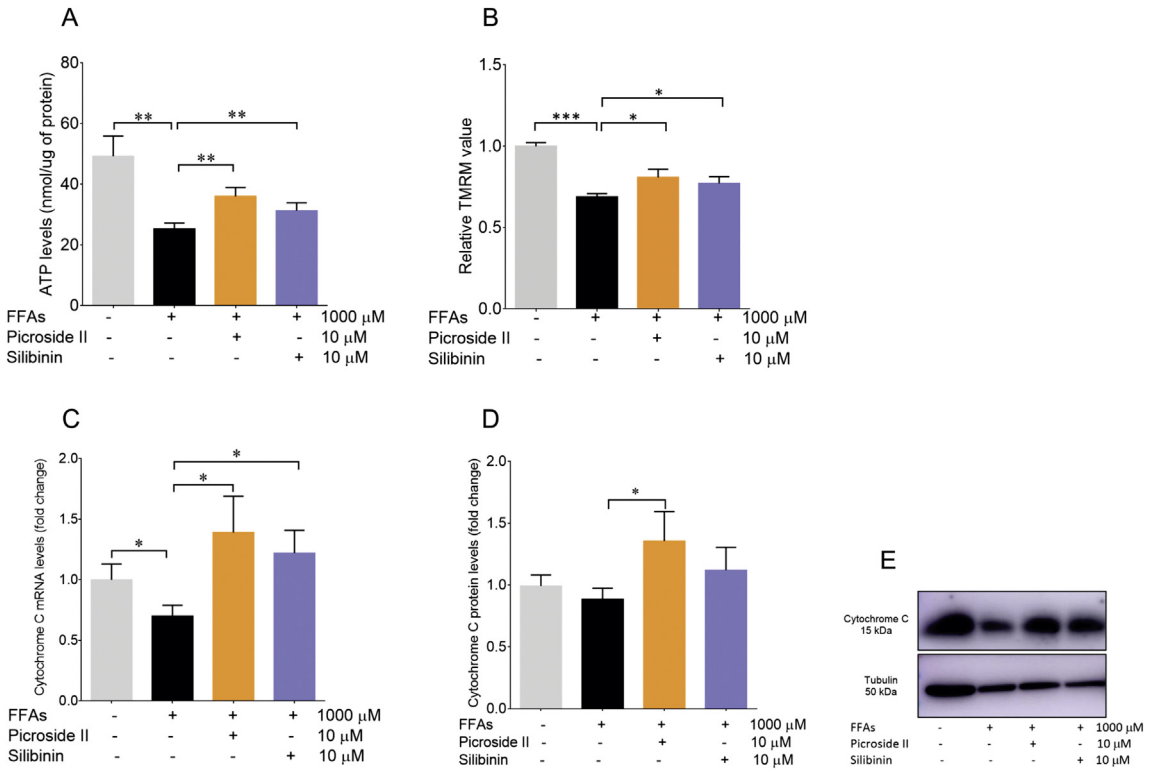

Fig. 4. Picroside II improves mitochondrial function: HepG2 cells were pre-treated with picroside II and silibinin at a concentration of 10 μM for 2 h, followed by FFAs – 1000 μM challenge for another 20 h. ATP determination using luciferase assay, FFAs – 1000 μM vs control $^{**}p < 0.01$, picroside II vs FFAs – 1000 μM $^{**}p < 0.01$ and silibinin vs control $^{**}p < 0.01$. ΔΨM was measured using TMRM, FFAs – 1000 μM vs control $^{***}p < 0.001$, picroside II vs FFAs – 1000 μM $^{*}p < 0.05$ and silibinin vs FFAs – 1000 μM, $^{*}p < 0.05$ (B). The RT-PCR analysis of Cytochrome C, picroside II vs FFAs- 1000 μM $^{*}p < 0.05$ (C) and Western blot analysis of Cytochrome C, picroside II vs FFAs –1000 μM, $^{*}p < 0.05$ (D and E). The values are expressed as mean ± SEM, N = 4, n = 3.

Several *in vitro* and *in vivo* studies, including the present one, have demonstrated an increase in the ROS production as a result of excess lipid accumulation within the hepatocytes [9]. Clinical studies have also reported an increase in lipid peroxidation in patients with NASH [33]. An increase in ROS generation can cause depletion of antioxidant enzymes (MnSOD, Catalase and glutathione peroxidase). This leads to formation of lipid peroxides having detrimental effects on hepatocytes [9]. In the present study, a significant decrease in the tGSH levels and a trend towards decrease in the GSH/GSSG ratio as well as antioxidant enzymes MnSOD and Catalase, was observed as a result of increased ROS formation.

In patients with NASH, an increase in the ROS is associated with impaired mitochondrial electron transport chain (ETC) and loss in the ΔΨm [34]. A decrease in ATP production, ΔΨm, and expression of Cytochrome C in FFAs-treated HepG2 cells suggest mitochondrial dysfunction. Animal models of mitochondrial dysfunction in NASH have shown alteration in the ETC complexes I, III, and IV [35]. In the present study, no effect of FFAs-loading was observed on the mRNA and protein expression of complex IV even though we observed a decrease in the ATP production. This suggests a need to explore the expression of complexes I and III since they are the major sites for superoxide formation [36–41]. Disruption in the complexes I and III has shown to increase formation of ROS, diminish tGSH, and deplete ATP generation [42]. Also, increase in the ROS is shown to damage mitochondrial DNA [43]. There were no changes observed in mRNA and protein expression of TFAM with FFAs treatment. This indicates that the degree of ROS did not damage the mitochondria to an extent to cause mitochondrial DNA damage.

Preventing the development of NASH with suitable safe phytomolecules would be hereby beneficial [44]. In the present study, the effects of picroside II, a phytoactive from *P. kurroa*, vis-à-vis silibinin, from *Silymarin marianum*, were examined on FFAs-induced lipotoxicity. Earlier, it was shown that picroside II significantly reduced fatty acid accumulation in HepG2 cells by decreasing the FFAs uptake and synthesis [18]. In the present study, besides attenuating lipid accumulation, picroside II also significantly decreased the ROS formation in FFAs-loaded HepG2 cells. This decrease in ROS formation was parallel to an increased expression of MnSOD and Catalase with picroside II pre-treatment. Picroside II also increased the levels of tGSH and GSH:GSSG. The decrease in ROS formation and increase in tGSH levels were comparable with silibinin pre-treatment. However, silibinin did not show any effect on the MnSOD and Catalase levels. Pre–clinical and clinical studies have shown anti-oxidant properties of silibinin [45]. Silibinin has shown to inhibit the formation of ROS by increasing tGSH, MnSOD, Catalase, and glutathione peroxidase levels in rat Kupffer cells, hepatocytes, HepG2 cells, and isolated rat hepatic mitochondria [46].

The present investigation also showed an improvement in mitochondrial function with picroside II. There was an increase in expression of Cytochrome C following picroside II pre-treatment. An increase in expression of Cytochrome C implies activation of its function as a single electron carrier in the electron transport chain catalyzing the reduction of oxygen molecule to water, thus leading to more ATP [34]. Picroside II was found to increase ΔΨm and ATP generation (Fig. 5A and B). Similarly, silibinin pre-treated group showed an increase in ΔΨm and ATP generation compared to FFAs-treated group.

The aforesaid evidence is significant so as to gain a deeper understanding of the mechanism of picroside II's activity in improving mitochondrial function. Excess of hepatic FFAs overload alters the

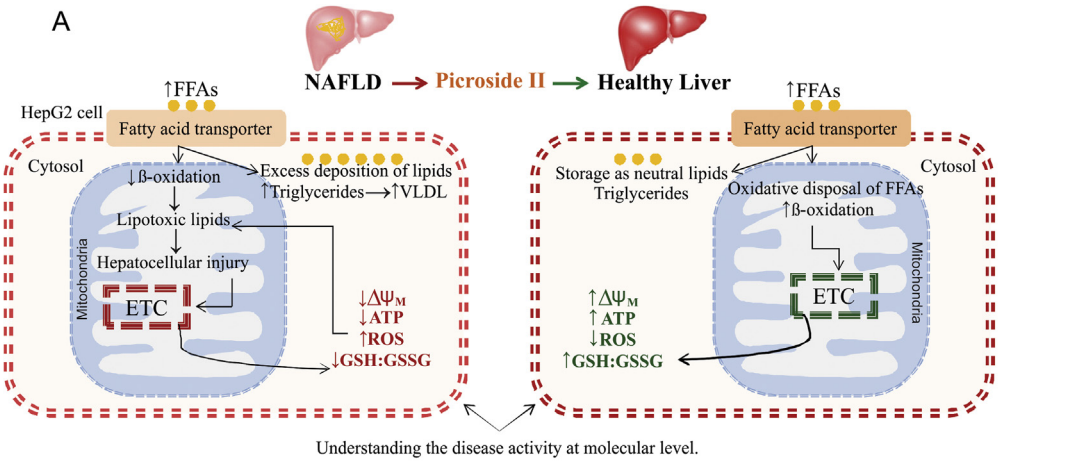

Note: $\Delta\Psi_M$ – mitochondrial membrane potential, ROS – reactive oxygen species, GSH – reduced glutathione, GSSG – oxidized glutathione.

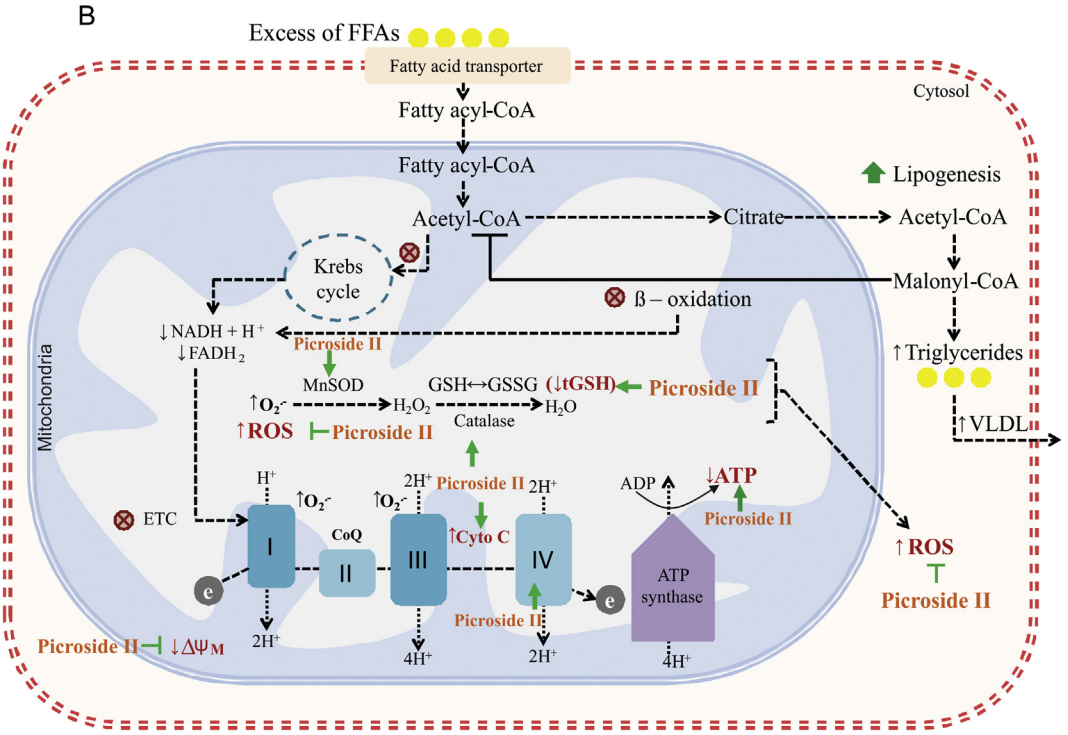

Fig. 5. Proposed model for picroside II's activity on FFAs-induced-lipotoxicity: Picroside II attenuates FFAs accumulation, decreases the production of ROS, and increases the levels of antioxidants (glutathione, MnSOD and Catalase). Picroside II also improves the mitochondrial functions by increasing the ATP production, decreasing the ΔΨM, and Cytochrome C expression (A and B).

process of β-oxidation, increasing the flow of reducing equivalents NADH and $FADH_2$ across ETC [38]. In the present study, picroside II significantly increased the ΔΨm and ATP levels. Also, in our study picroside II was found to increase the mRNA levels of COX IV in FFAs-loaded cells. Besides complex IV, there is a need to study the effect of picroside II on complexes I and III for its activity on ETC.

5. Conclusion

The current *in vitro* fatty liver model has explored the activity of picroside II on fatty acid accumulation, oxidative stress, and mitochondrial function. Besides picroside II, there are many other active compounds present in *P. kurroa*. These include picroside I and apocynin whose activities have not been explored on other targets involved in pathogenesis of NAFLD such as insulin resistance, altered lipid metabolism, lipotoxicity, oxidative stress and inflammation, activation of immune cells, apoptosis, necrosis, fibrogenesis, and collagen turnover [46]. Hence, in addition to studying picroside II, it will be desirable to study *P. kurroa* or fortify it with picroside II for its activity in NAFLD.

The pathogenesis of NAFLD also comprises of several other dynamic pathways and cross-talks between two or more cell types in liver [47]. Primary hepatocytes have been proposed as a standard model for studying mechanisms of molecular activity of a compound. But in view of the earlier clinical and *in vitro* activities shown by *P. kurroa* and picroside II, these results in HepG2 cells gain relevance [48]. The effect of FFAs-induced-lipotoxicity in hepatocytes can be followed up in other models viz., hepatic spherules,

dual cell cultures with Kupffer cells or primary hepatocytes, etc [49]. Further pre-clinical and toxicity studies can be explored for the enriched extract of *P. kurroa* as a phytopharmaceutical or picroside II as a new chemical entity.

Source(s) of funding

Department of Science & Technology, Government of India, under Women Scientist-A program, SR/WOS-A/LS-1135/2014

Conflict of interest

None

Author contributions

Conceptualization, Hiteshi Dhami-Shah, Ullas Kolthur-Seetharam and Ashok Vaidya; Investigation, Hiteshi Dhami-Shah (for Cell culture, ORO staining, MTT assay, ROS and ATP determination, measurement of ΔΨM, RT-PCR and Western blot), Manasi Talwadekar (for measurement of ΔΨm), Eisha Shaw (for ATP determination); Original draft, Hiteshi Dhami- Shah, Ashok Vaidya, Ullas Kolthur-Seetharam, Manasi Talwedekar, Eisha Shaw, Rama Vaidya and Shobha Udipi; Funding acquisition, Hiteshi Dhami-Shah; Supervision, Ullas Kolthur-Seetharam and Ashok Vaidya.

Acknowledgements

We thank Department of Science & Technology, Government of India, for the research grant under Women Scientist-A program, SR/WOS-A/LS-1135/2014.

Appendix A. Supplementary data

Supplementary data to this article can be found online at https://doi.org/10.1016/j.jaim.2021.04.007.

References

[1] Angulo P. Nonalcoholic fatty liver disease. N Engl J Med 2002;346(16):1221–31.
[2] Dowman JK, et al. Pathogenesis of non alcoholic fatty liver disease. Q J Med 2010;103:71–83. 2010.
[3] Matteoni CA, Younossi ZM, Gramlich T, Boparai N, Liu YC, McCullough AJ. Nonalcoholic fatty liver disease: a spectrum of clinical and pathological severity. Gastroenterology 1999;116(6):1413–9.
[4] Younossi Zobair, Anstee Quentin M, Marietti Milena, et al. Global burden of NAFLD and NASH: trends, predictions, risk factors and prevention. Nat Rev Gastroenterol Hepatol 2018;(15):11–20.
[5] Sanyal AJ. Mechanisms of disease. Pathogenesis of nonalcoholic fatty liver disease. Nat Clin Pract Gastroenterol Hepatol 2005;2:46–53.
[6] Sumida Y, Niki E, Naito Y, Yoshikawa T. Involvement of free radicals and oxidative stress in NAFLD/NASH. Free Radic Res November 2013;47(11):869–80.
[7] Cohen JC, Horton JD, Hobbs HH. Human fatty liver disease: old questions and new insights. Science 2011;332(6037):1519–23.
[8] Day CP, James OF. Steatohepatitis: a tale of two hits. Gastroenterology 1998;114(4):842–5. 1998.
[9] Rolo AP, Teodoro JS, Palmeira CM. Role of oxidative stress in the pathogenesis of nonalcoholic steatohepatitis. Free Radic Biol Med 2012;52(1):59–69.
[10] Tolman KG, Dalpiaz AS. Treatment of non-alcoholic fatty liver disease. Therapeut Clin Risk Manag 2007;3(6):1153–63.
[11] Acharya JT. Charak samhita. Chakrapani tika, choukhambha sanskrut sansthan. 5th edi. 2001. Varanasi.
[12] Antarkar DS, Tathed PS, Vaidya AB. A pilot phase II trial with Arogyawardhini and Punarnavadi kwath in viral hepatitis. Panminerva Med 1978;20:157–63.
[13] Dwivedi Y, Rastogi R, Ramesh C, Sharma SK, Kapoor NK, Garg NK, et al. Hepatoprotective activity of Picroliv against carbon tetrachloride induced liver damage in rats. Indian J Med Res 1990;92b:195–200.
[14] Dwivedi Y, Rastogi R, Garg NK, Dhawan BN. Prevention of paracetamol-induced hepatic damage in rats by Picroliv, the standardized active fraction from Picrorhiza kurroa. Phytother Res 1991;5:115–9.
[15] Dwivedi Y, Rastogi R, Sharma SK, Garg NK, Dhawan BB. Picroliv affords protection against thioacetamide-induced hepatic damage in rats. Planta Med 1991;57:25–8.
[16] Visen PK, Shukla B, Patnaik GK, Dhawan BN. Prevention of galactosamine-induced hepatic damage by Picroliv: study on bile flow and isolated hepatocytes. Planta Med 1993;59:37–41.
[17] Shetty SN, Mengi S, Vaidya R, Vaidya AD. A study of standardized extracts of Picrorhiza kurroa Royle ex Benth in experimental non-alcoholic fatty liver disease. J Ayurveda Integr Med 2010;1:203–10.
[18] Dhami-Shah H, Vaidya R, Udipi S, Raghavan S, Abhijit S, Mohan V, et al. Picroside II attenuates fatty acid accumulation in HepG2 cells via modulation of fatty acid uptake and synthesis. Clin Mol Hepatol 2018;24(1):77–87.
[19] Cousin Sharon P, Sigrun R Hugl, Wrede Christian E, Kajio Hiroshi, Meyers Martin G, Rhodes Christopher J. Free fatty acid induced inhibiton of glucose and insulin like growth factor-1 induced deoxyribonucleic acid synthesis in the the pancreatic β-cell line INS-1. Endocrinology 2000;142(1):229–40.
[20] Mosmann T. Rapid colorimetric assay for cellular growth and survival: application to proliferation and cytotoxicity assays. J Immunol Methods 1983;65:55–63.
[21] Kraus NA, Ehebauer F, Zapp B, Rudolphi B, Kraus BJ, Kraus D. Quantitative assessment of adipocyte differentiation in cell culture. Adipocyte 2016;5(4):351–8.
[22] Eruslanov E, Kusmartsev S. Identification of ROS using oxidized DCFDA and flow-cytometry. Methods Mol Biol 2010;594:57–72.
[23] Rahman Irfan, Kode Aruna, Biswas Saibal K. Assay for quantitative determination of glutathione and glutathione disulfide levels using enzymatic recycling method. Nat Protoc 2006;6:3159–65.
[24] Bradford MM. A rapid and sensitive method for the quantitation of microgram quantities of protein utilizing the principle of protein-dye binding. Anal Biochem 1976;72:248–54.
[25] De Rautlin De La Roy Y, Messedi N, Grollier G, Grignon B. Kinetics of bactericidal activity of antibiotics measured by luciferin-luciferase assay. J Biolumin Chemilumin 1991;6(3):193–201.
[26] Distelmaier Felix, Werner J, Koopman H, Testa Epifania R, de Jong Arjan S, Swarts Herman G, et al. Life cell quantification of mitochondrial membrane potential at the single organelle level. Cytometry 2008;73A:129–38.
[27] Zanoni Ivan, Ostuni Renato. mRNA expression analysis by real-time PCR. Protocol Exchange 2009;139.
[28] Mahmood T, Yang P-C. Western blot: technique, theory, and trouble shooting. N Am J Med Sci 2012;4(9):429–34.
[29] Varghes L, Agarwal C, Tyagi A, Singh RP, Agarwal R. Silibinin efficacy against human hepatocellular carcinoma. Clin Canc Res 2005;11(23):8441–8.
[30] Ucar Fatma, Sezer Sevilay, Erdogan Serpil, Akyol Sumeyya, Armutcu Ferah, Akyol Omer. The relationship between oxidative stress and nonalcoholic fatty liver disease: its effects on the development of nonalcoholic steatohepatitis. Redox Rep 2013;18(4):127–33.
[31] Masarone M, Rosato V, Dallio M, et al. Role of oxidative stress in pathophysiology of nonalcoholic fatty liver disease. Oxid Med Cell Longev 2018;2018:9547613.
[32] Pessayre D, Fromenty B. NASH: a mitochondrial disease. J Hepatol 2005;42(6):928–40.
[33] Chalasani N, Deeg MA, Crabb DW. Systemic levels of lipid peroxidation and its metabolic and dietary correlates in patients with nonalcoholic steatohepatitis. Am J Gastroenterol 2004;99(8):1497–502.
[34] Begriche K, Igoudjil A, Pessayre D, Fromenty B. Mitochondrial dysfunction in NASH: causes, consequences and possible means to prevent it. Mitochondrion 2006;6(1):1–28.
[35] Rector RS, Thyfault JP, Uptergrove GM, Morris EM, Naples SP, Borengasser SJ, et al. Mitochondrial dysfunction precedes insulin resistance and hepatic steatosis and contributes to the natural history of nonalcoholic fatty liver disease in an obese rodent model. J Hepatol 2010;52:727–36.
[36] Escobar JA, Rubio MA, Lissi EA. Sod and catalase inactivation by singlet oxygen and peroxyl radicals. Free Radic Biol Med 1996;20(3):285–90.
[37] Hüttemann M, Pecina P, Rainbolt M, et al. The multiple functions of cytochrome c and their regulation in life and death decisions of the mammalian cell: from respiration to apoptosis. Mitochondrion 2011;11(3):369–81.
[38] Fromenty B, Pessayre D. Inhibition of mitochondrial beta-oxidation as a mechanism of hepatotoxicity. Pharmacol Ther 1995;67:101–54.
[39] Perez-Carreras M, Del Hoyo P, Martin MA, Rubio JC, Martin A, Castellano G, et al. Defective hepatic mitochondrial respiratory chain in patients with nonalcoholic steatohepatitis. Hepatology 2003;38:999–1007.

[40] Brand MD, Nicholls DG. Assessing mitochondrial dysfunction in cells. Biochem J 2011;435(2):297–312.
[41] García-Ruiz I, Solís-Muñoz P, Fernández-Moreira D, Grau M, Colina F, Muñoz-Yagüe T, et al. High-fat diet decreases activity of the oxidative phosphorylation complexes and causes nonalcoholic steatohepatitis in mice. Dis Model Mech 2014 Nov;7(11):1287–96.
[42] Simões ICM, Fontes A, Pinton P, Zischka H, Wieckowski MR. Mitochondria in non-alcoholic fatty liver disease. Int J Biochem Cell Biol 2018;95:93–9.
[43] Begriche Karima, Igoudjil Anissa, Pessayre Dominique, Fromenty Bernard. Mitochondrial dysfunction in NASH: causes, consequences and possible means to prevent it. Mitochondrion 2006;6:1–28.
[44] Perumpail BJ, Li AA, Iqbal U, et al. Potential therapeutic benefits of herbs and supplements in patients with NAFLD. Diseases 2018;6(3):80.
[45] Surai PF. Silymarin as a natural antioxidant: an overview of the current evidence and perspectives. Antioxidants 2015;4(1):204–47.
[46] Loguercio C, Festi D. Silybin and the liver: from basic research to clinical practice. World J Gastroenterol 2011;17:2288–301.
[47] Garcia-Ruiz I, Fernandez-Moreira D, Solis-Munoz P, Rodriguez-Juan C, DiazSanjuan T, Munoz-Yague T, et al. Mitochondrial complex I subunits are decreased in murine nonalcoholic fatty liver disease: implication of peroxynitrite. J Proteome Res 2010;9:2450–9.
[48] Chavez-Tapia NC1, Rosso N, Tiribelli C. In vitro models for the study of non-alcoholic fatty liver disease. Curr Med Chem 2011;18(7):1079–84.
[49] Cole Banumathi K, Feaver Ryan E, Wamhoff Brian R, Dash Ajit. Non-alcoholic fatty liver disease (NAFLD) models in drug discovery. Expet Opin Drug Discov 2018;13:193–205.